MAGNETIC FIELD MEASUREMENT OF QUADRUPOLE MAGNETS FOR S-LSR

T. Takeuchi, K. Noda, S. Shibuya, National Institute of Radiological Science, 4-9-1, Inage-Ku, Chiba-shi, 263-8555, Chiba, Japan
A. Noda, T. Shirai, H. Tongu, H. Fadil, M. Ikegami, Institute for Chemical Research, Kyoto University, Gokashou, Uji-shi, 611-0011, Kyoto, Japan

Abstract

The magnetic field measurement of the quadrupole magnet for the compact ion storage ring, S-LSR, is presented. To investigate the magnetic flux at the interspace of the quadrupole (QM) and bending magnet (BM), the QM magnet field measurement by a Hall probe is carried out together with the field clamp and BM for S-LSR The direct measurement of the integrated field gradient error by the twin coil is studied. Then, obtained results by using twin coil (the horizontal distribution of the integrated field gradient and the higher order coefficients) will be presented.

QUADRUPOLE MAGNETS FOR S-LSR

S-LSR is a low energy ion storage/cooler ring consisting of a circumference of 22.557 meters, a superperiodicity of 6, a straight section length of 1.86 meters, and a magnet rigidity of 1.0 Tm. The scientific programs for S-LSR are an electron cooling of a laser-produced ions and a realization of a crystal ion beam [1].

S-LSR has 12-QM's with a bore radius of 70 mm, a maximum field gradient of 5 T/m, and a magnet length of 200 mm. By requirements for the small ring accelerator, distances between accelerator components at the arc sections are very short as shown in Fig.1 (a). The distance between a bending magnet and QM is 200 mm. To suppress and control a magnetic flux in a fringing field of a BM, a field clamp with a thickness of 25 mm was installed in between BM and QM. The distance between the field clamp and QM is 80 mm. as shown in Fig. 1 (b). The 3D calculation for QM represented that the QM field is strongly influenced by the field clamp. Therefore, QMs were designed and optimized in considering the influence of the field clamp [2]. Table 1 lists the specifications of QM for S-LSR.

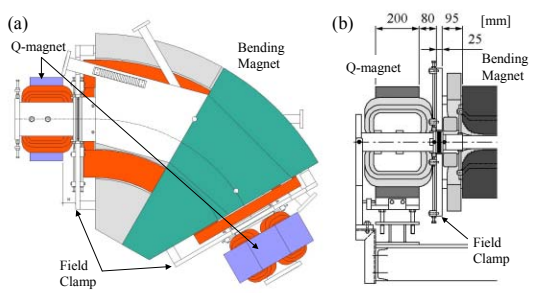

Fig. 1. (a) Magnet location at the arc section in S-LSR. (b) The distance between the bending magnet (BM) and the quadrupole magnet (QM) is 200 mm. distance between BM and field clamp is 95 mm which is occupied by the BM conductor. A thickness of the field clamp is 25 mm. The distance between the field clamp and QM is 80 mm which is also occupied by the QM conductor.

Table 1: Specifications of quadrupole magnets for S-LSR

Maximum field strength	5 [T/m]
Bore radius	70 [mm]
Magnet length	200 [mm]
Ampere turns	9800 [A Turn]
Maximum current density	350 [A]
The number of QM	12

HALL PROBE MEASUREMENT

A QM magnet field measurement by a Hall probe was carried out together with the field clamp and BM for S-LSR. The measurement system consists of three-axis movable stage, a temperature controlled Hall probe (Group3: DTM-151-DG, Probe head: MPT-141), and an automatic data-analyzing system. The mapping area covers a plane of –300~+300 mm for the longitudinal axis (z-axis) and –100~+100 mm for the horizontal axis (x-axis). The position of Z = 0 mm corresponds to the center of the magnet length of the QM for S-LSR. The overall view of the magnetic field measurement is shown in Fig.2.

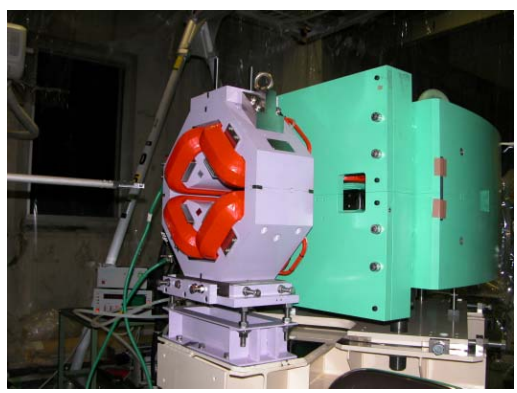

Fig.2. The overall view of the magnetic field measurement for the BM and the QM for S-LSR.

Figure 3 (a) and (b) show the horizontal distribution of the integrated field gradient error for the conditions of without and with the BM and the field clamp, respectively.

These results seem that the existence of the BM and the field clamp caused the increasing of the integrated field gradient error in the horizontal outer region.

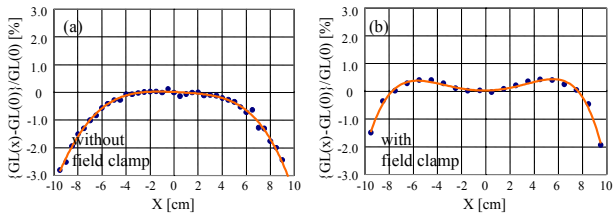

Fig. 3 (a): The measured horizontal distribution of the integrated field gradient error for the QM for S-LSR. The solid curve is a fitted polynomial curve of 6th degree. The excitation current is 200 A. (b): The the horizontal distribution of the integrated field gradient error. The excitation currents for the BM and QM for S-LSR are 0A and 200A, respectively.

For an interspace of BM and QM, the superposition of the magnetic flux from each magnets was investigated. From 3 measurements in the excitation of only BM, QM and both BM and QM, it is found that the magnetic field by both of BM and QM can be expressed with the sum of magnetic filed for the excitation of a respective magnet. Therefore, the saturation of the field clamp is no influence for the magnetic field in the beam existence region (horizontal: ± 100 mm, vertical: ± 15 mm). This means that it is possible to perform the independent measurement for BM or QM.

The measured excitation curve of the QM states that the influence of the saturation at the maximum current of 350 A is less than 1 % [3].

LONG COIL MEASUREMENT

For the measurement of the field gradient, Hall probe mapping suffers the error from the subtraction of mapping data. Also, the Hall planer effect by the inhomogeneous magnetic field reduces the accuracy of the measurement. Therefore, we prepared a measurement system using a long coil as shown in Fig. 4.

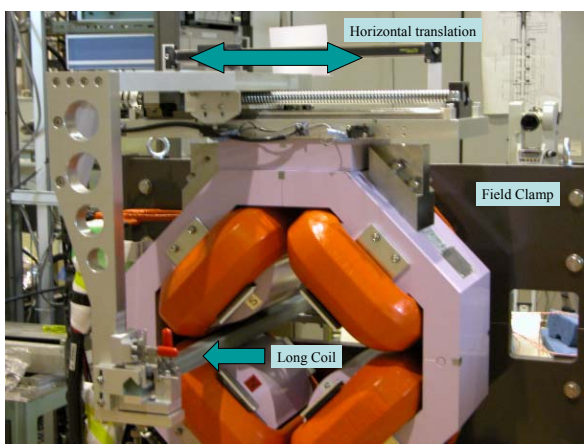

Fig. 4. The long coil measurement system, QM and the field clamp.

In this system, the induced voltage by moving the coil to the horizontal direction is stored by the integrated circuit (480 Fluxmeter, LakeShore). We can realize the direct measurement of the field gradient and measure the outer region on horizontal direction (x ~ ± 110mm). In addition, the method by the twin coil can measure the difference of the field gradient directly [4,5]. Figure 5 (a) shows the dimension of the twin coil. The number of turn is 700 and the length is 600 mm.

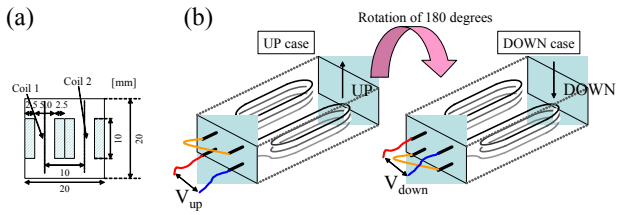

Fig. 5 (a):The dimension of the twin coil. (b): Schematic drawing of the twin coil polarity (UP and DOWN). The number of turn is 700 and the length is 600 mm.

The induced voltage by moving long coil can be written by

$$V_1 = CNA_1 \int \left.\frac{dBy}{dx}\right|_{x_1} ds\ \Delta x\,, \qquad (1)$$

where C is calibration constant of the circuit, N and A_1 are the turn number and the effective area of a coil, Δx is the moving length. In cases as drawn in Fig. 5 (b), induced voltages are given by

$$V_{up} = CN\left[A_1 \int \left.\frac{dBy}{dx}\right|_{x_1} - \int A_2 \left.\frac{dBy}{dx}\right|_{x_2}\right] ds \cdot \Delta x \qquad (2)$$

$$V_{down} = -CN\left[A_1 \int \left.\frac{dBy}{dx}\right|_{x_2} - A_2 \int \left.\frac{dBy}{dx}\right|_{x_1}\right] ds \cdot \Delta x\,, \qquad (3)$$

where x_1 and x_2 are the initial position of coil 1 and 2. Adding up Eq. (2) and (3), the following relation is obtained;

$$V_{twin} = V_{up} + V_{down} = CN\Delta x(A_1 + A_2)\left(\int \left.\frac{dBy}{dx}\right|_{x_1} - \int \left.\frac{dBy}{dx}\right|_{x_2}\right) ds\,, \qquad (4)$$

$$= CN\Delta x(A_1 + A_2)\int \frac{d^2By}{dx^2} ds\,\delta x$$

where $\delta x = 10\,[mm]$ is the distance between each coils. On the other hand, the sum of measured results with single coil is presented in

$$V_{\sin gle} = V_1 + V_2 = CN\Delta x(A_1 + A_2)\int \left.\frac{dBy}{dx}\right|_{x=0} ds\,. \qquad (5)$$

From (4) and (5), the differentiation for the horizontal distribution of the field gradient error is derived;

$$\frac{\int \frac{d^2By}{dx^2} ds}{\int \left.\frac{dBy}{dx}\right|_{x=0} ds} = \frac{1}{\delta x}\frac{V_{twin}}{\left.V_{\sin gle}\right|_{x=0}}\,. \qquad (6)$$

Figure 6 shows the horizontal distribution for the left hand of the equation (6) on the condition of the current of 200A.

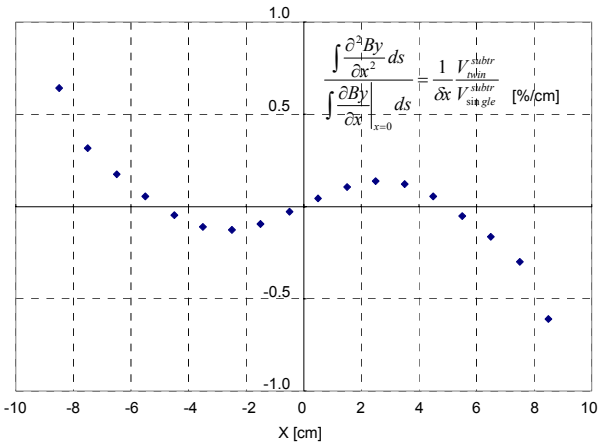

Fig. 6. The horizontal distribution for the differentiation of the field gradient error.

The integrated field gradient of QM can be expanded as

$$G_{(x)}L = \frac{dBy}{dx} = G_0L\{1 + a_1(\frac{x}{r_0}) + a_2(\frac{x}{r_0})^2 + a_3(\frac{x}{r_0})^3 + \cdots\}. \quad (7)$$

where $G_0L \equiv \int \left.\frac{dBy}{dx}\right|_{x=0} ds$ is the integrated field gradient at QM centre. By differentiating Eq. (7),

$$G'_{(x)}L = \int \frac{d^2By}{dx^2} ds = \frac{G_0L}{r_0}\{a_1 + 2a_2(\frac{x}{r_0}) + 3a_3(\frac{x}{r_0})^2 + 4a_4(\frac{x}{r_0})^3 + \cdots\} \quad (8)$$

is derived. The coefficients, a_i, are dimensionless and are written as $a_i = \frac{r_0^i}{i!}\frac{d^iGL}{dx^i}$. The relation (6) is rewritten by using Eq. (7) and (8) as;

$$\frac{V_{twin}}{\left.V_{single}\right|_{x=0}} = \frac{\frac{G_0L}{r_0}\left[a_1 + 2a_2(\frac{x}{r_0}) + 3a_3(\frac{x}{r_0})^2 + 4a_4(\frac{x}{r_0})^3 + \cdots\right]}{G_{(0)}L}\delta x. \quad (9)$$

The higher order coefficients are obtained by fitting the measured data (Fig. 6) with the right hand side of Eq. (9). The results are listed in Table 2. Substituting these coefficients, the horizontal distribution of the integrated field gradient error can be obtained. The integrated field gradient error with the twin coil measurement is shown in Fig. 7. The integrated field gradient is better than ± 1 % in the horizontal region of x = -95 ~ +95 mm. The excitation current is 200A.

Table 2: The higher order coefficients of the polynomial expansion of the integrated field gradient obtained by fitting to the measured data with the twin coil.

a1 (sextupole)	5.1232E-04	a5	8.5642E-04
a2 (octupole)	1.5742E-02	a6	-2.1843E-02
a3	-5.4850E-04	a7	-6.6123E-04
a4	-8.4623E-03		

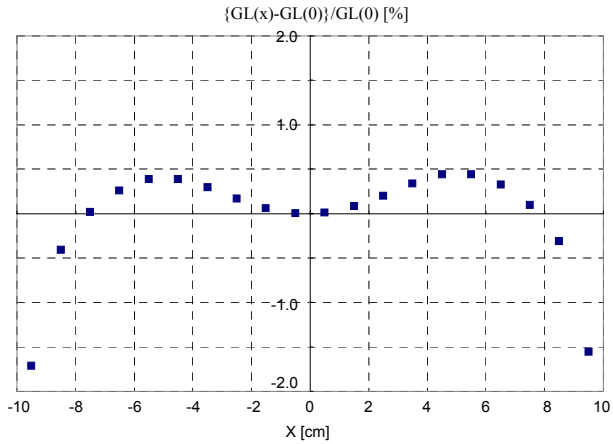

Fig. 7. The horizontal distribution of the integrated field gradient error by the twin coil measurement.

CONCLUSION

We described the magnetic field measurement of QM for S-LSR. The QM magnetic field measurement together with the BM and the field clamp was performed by Hall probe. The results show that the existence of the BM and the field clamp increases the integrated field gradient error in the horizontal outer region. From the investigation of the superposition of the magnetic flux from BM and QM, we found it is possible to perform the independent measurement for BM or QM. The direct measurement of the integrated field gradient error by the twin coil was carried out. By this, the integrated field gradient in a good accuracy was obtained. The twin coil measurement of 12 QM's is remained as next step.

REFERENCES

[1] A.Noda, et al., Proc. of the Workshop on Ion Beam Cooling - Toward the Crystalline Beam, World Scientific Publishing Co. Pte. Ltd, 2002, p. 3.

[2] T. Takeuchi, et al., " Optimization of lattice quadrupole magnets for cooler ring, S-LSR ", Accepted to Nuclear Instruments and Methods in Physics Research, NIM A.

[3] Takeshi Takeuchi, et al., " Design and Measurement of the S-LSR Quadrupole Magnet considering the Influence of a Neighboring Field Clamp", Accepted to IEEE Transactions on Applied Superconductivity.

[4] M. Kumada, et al., Proc. of 2nd Symp. on Acc. Sci. & Tech. (1978) p. 73.

[5] A.Noda, et al., "Quadrupole Magnet for TARN", INS-NUMA-23 (1980).